Supporting Information

Mononuclear Manganese(III) Superoxo Complexes: Synthesis, Characterization and Reactivity

Yen-Hao Lin,[†] Hanna Hinrika Cramer,[‡] Maurice van Gastel,[⊥] Yi-Hsuan Tsai,[†] Chi-Yi Chu,[†] Ting-Shen Kuo,[#] I-Ren Lee,*[,†] Shengfa Ye,*[,⊥] Eckhard Bill,*[,‡] and Way-Zen Lee*[,†]

[†]Department of Chemistry, National Taiwan Normal University, Taipei 11677, Taiwan

[‡]Department of Molecular Theory and Spectroscopy, Max-Planck-Institut für Chemische Energiekonversion, Mülheim an der Ruhr D-45470, Germany

[⊥]Department of Molecular Theory and Spectroscopy, Max-Planck-Institut für Kohlenforschung, Mülheim an der Ruhr D-45470, Germany

[#]Instrumentation Center, Department of Chemistry, National Taiwan Normal University, Taipei 11677, Taiwan

*Corresponding author. Email: wzlee@ntnu.edu.tw (W.-Z.L); shengfa.ye@kofo.mpg.de (S.Y.); eckhard.bill@cec.mpg.de (E.B.); irenlee@ntnu.edu.tw (I.-R.L)

Contents

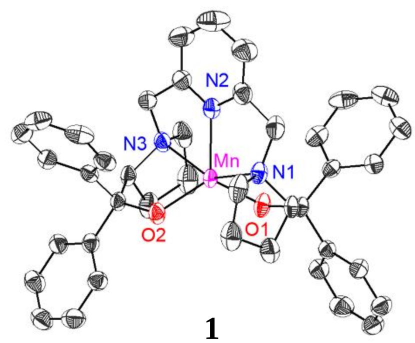

1

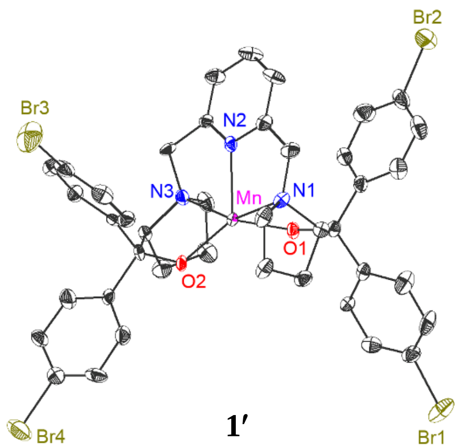

1′

Figure S1. ORTEP presentation of Mn(BDPP) (**1**) and Mn(BDP^{Br}P) (**1′**). Hydrogen atoms are omitted for clarity.

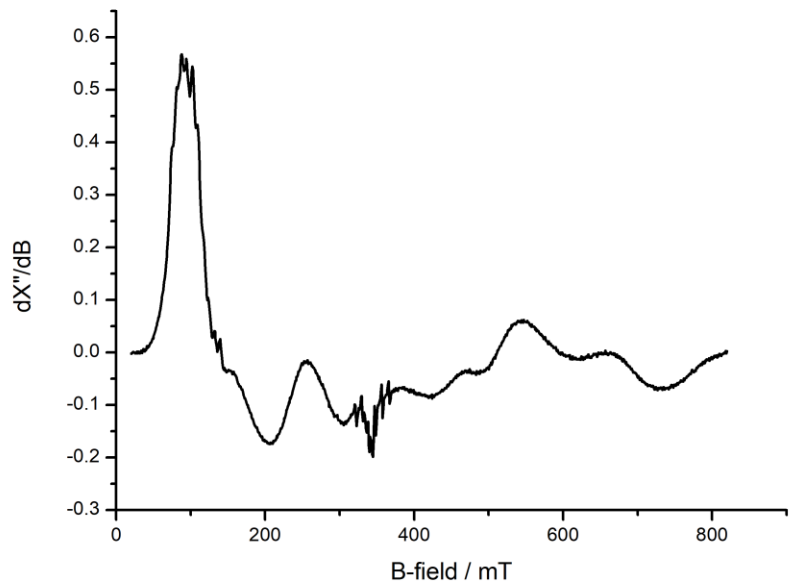

Figure S2. EPR spectrum of **1** (1 mM) in MeTHF recorded at 10 K. (Frequency 9.65629 GHz, power 0.2 mW, modulation 100 kHz/0.75 mT)

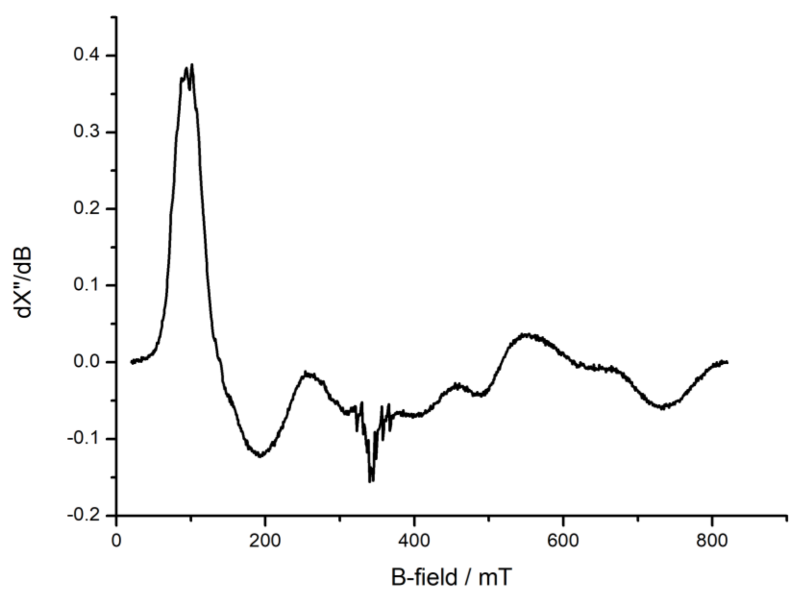

Figure S3. EPR spectrum of **1′** (1 mM) in MeTHF recorded at 10 K. (Frequency 9.65864 GHz, power 0.2 mW, modulation 100 kHz/0.75 mT)

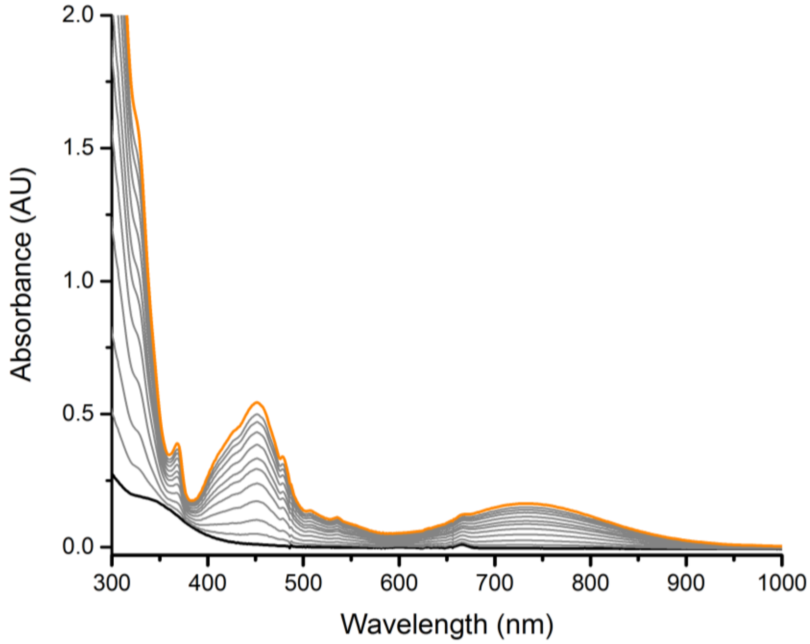

Figure S4. UV-vis spectra of **1** (black, 0.4 mM) reacting with O_2 forming **2** (orange, 0.4 mM) in THF at −80 °C.

(a)

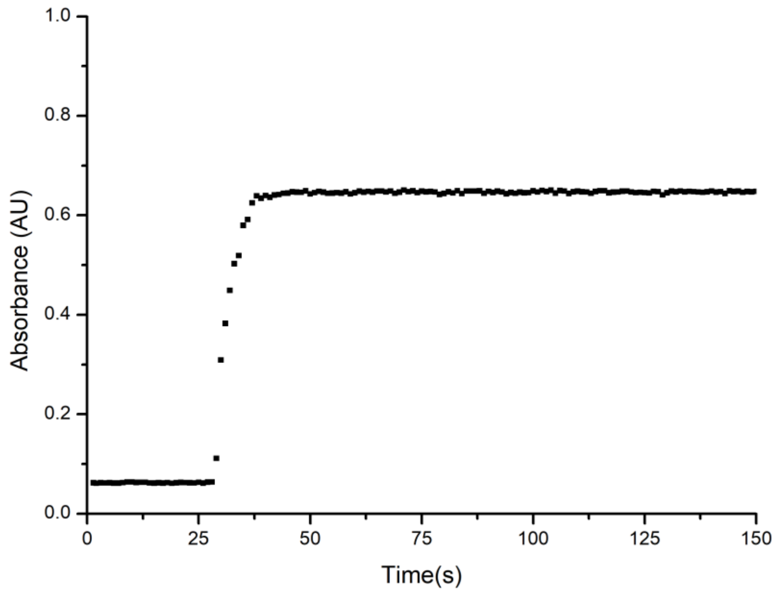

(b)

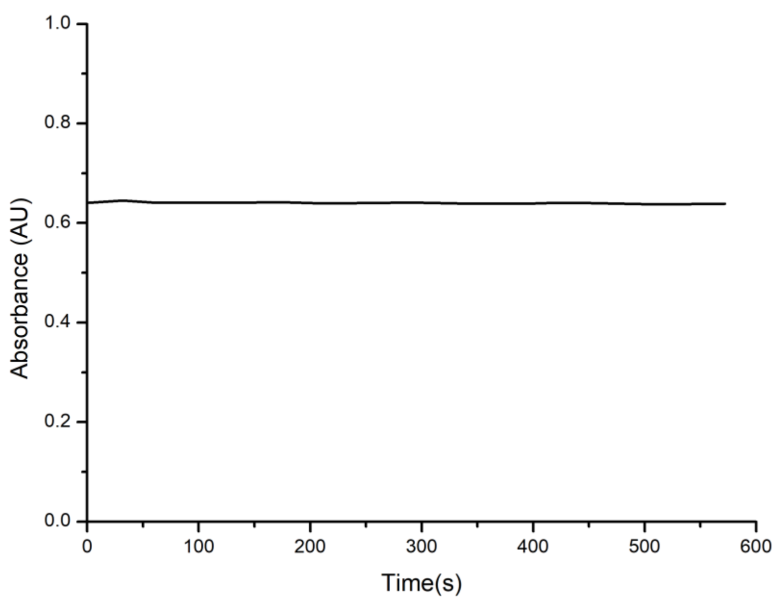

Figure S5. (a) The trace of formation of **2′** (0.4 mM) by bubbling O_2 into a THF solution of **1** from the monitoring for the absorption band at 450 nm; (b) The trace of retention of **2′** in THF (0.4 mM) from purging the solution with argon for 10 mins at −80 °C.

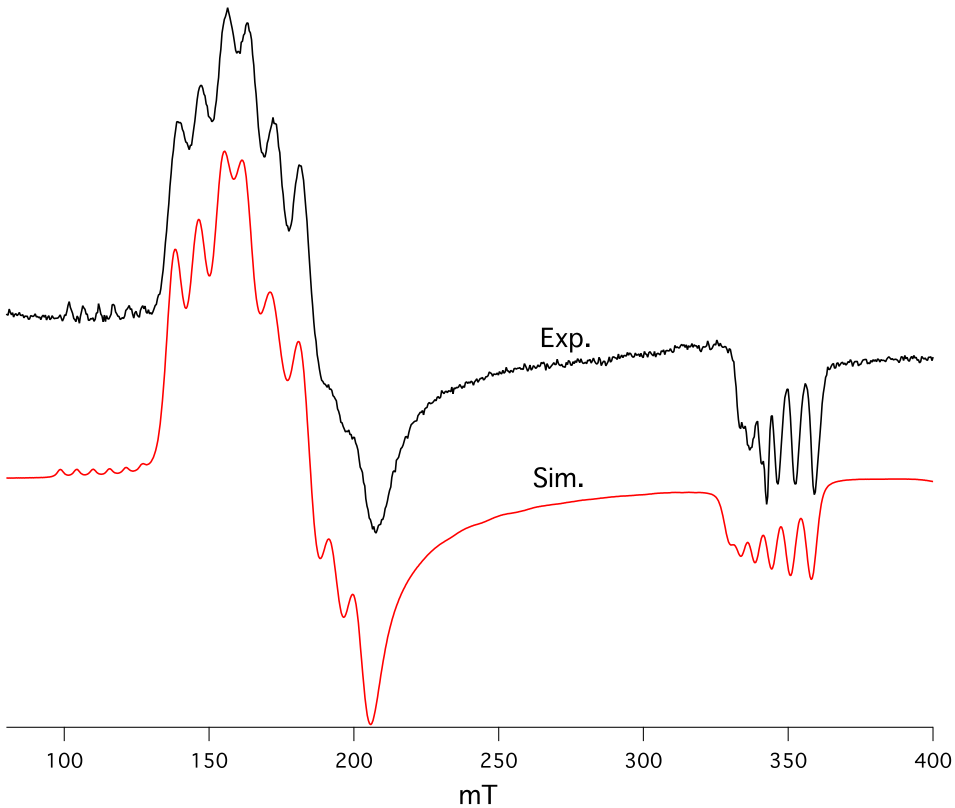

Figure S6. EPR spectrum of **2** (1 mM) recorded at 10 K. (Frequency 9.655 GHz, power 0.2 mW, modulation 100 kHz/0.75 mT). The simulation was obtained by the following parameter, g_{iso} = 1.997(10), D = –5.4(5) cm^{-1}, E/D = 0.05(1), and $|A_{x,y,z}|$ = 237(10), 223(10), 158(10) MHz. The spin concentration of the superoxo complex with S = 3/2 was determined two different samples to be ca. 95 and 99 % of the chemical concentration (2 mM), with ca. ±10% error. To this end, the prominent subspectrum from the 'allowed' transitions within the excited Kramers doublet ($m_s = \pm 1/2$) with effective g values at 4 and 2 was numerically double-integrated in the field range 130 – 380 mT, and compared with the integrated spectrum of a 1mM Cu(II) standard measured at non-saturating conditions (30 K, 0.05 mW). Both spectra were corrected for different Aasa-Vanngard factors for field-swept spectra, arising from different (effective) g values.[1] In addition, the $m_s = \pm 1/2$ subspectrum of the target compound 2 was corrected for the corresponding Boltzmann factor of the excited state by using D = -5.2 cm^{-1} taken form the analysis of the temperature variation described in the main text.

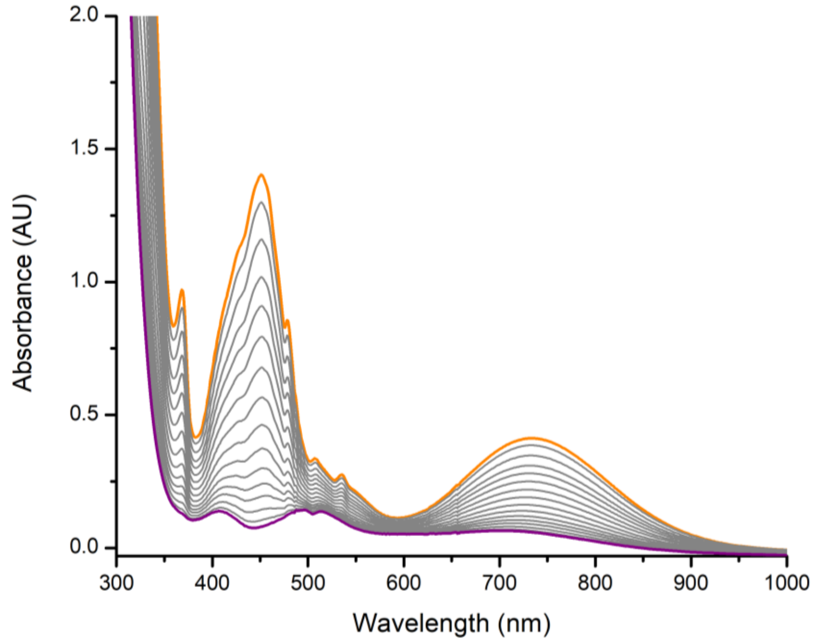

Figure S7. UV-vis spectra of **2** (orange line, 1 mM) reacting with 10 equivalents of TEMPOH in THF at −90 °C. Purple line represents Mn^{III}(BDPP)(OOH) (**5**) with four absorption bands at 410, 495, 515 and 720 nm.

(a) (b)

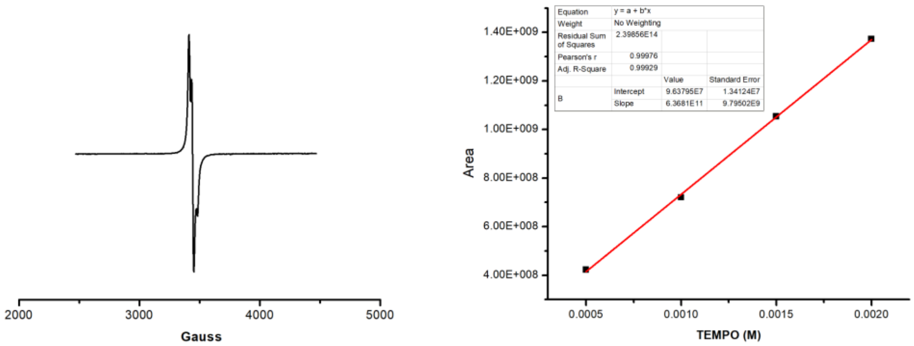

Figure S8. (a) EPR signal (g = 2.006, 77K) of the produced TEMPO radical (integrated area: 6.5×10^8, 86% vs calibration) obtained from the reaction of **2** (1.0×10^{-3} M) with 10 equivalents of TEMPOH at −90 °C; (b) the calibration curve of TEMPO radical.

(a) (b)

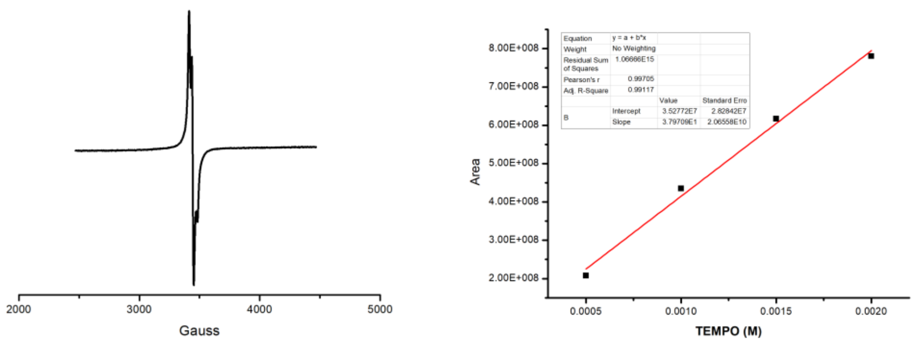

Figure S9. (a) EPR signal (g = 2.006, 77K) of the produced TEMPO radical (integrated area: 3.8×10^8, 93% vs calibration) obtained from the reaction of **2′** (1.0×10^{-3} M) with 10 equivalents of TEMPOH at −90 °C; (b) the calibration curve of TEMPO radical.

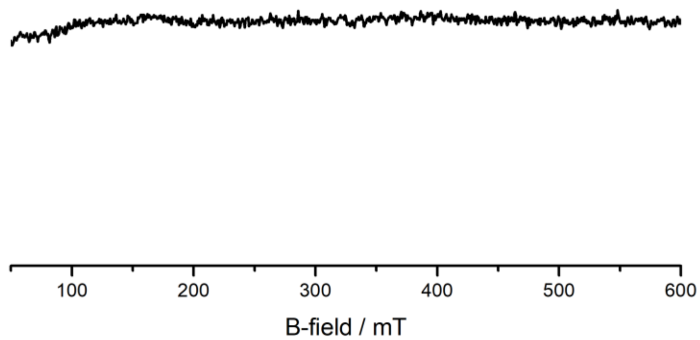

Figure S10. EPR spectrum of **6’** (1 mM) recorded at 10 K. (Frequency 9.388 GHz, power 0.2 mW, modulation 100 kHz/0.75 mT).

(a)

(b)

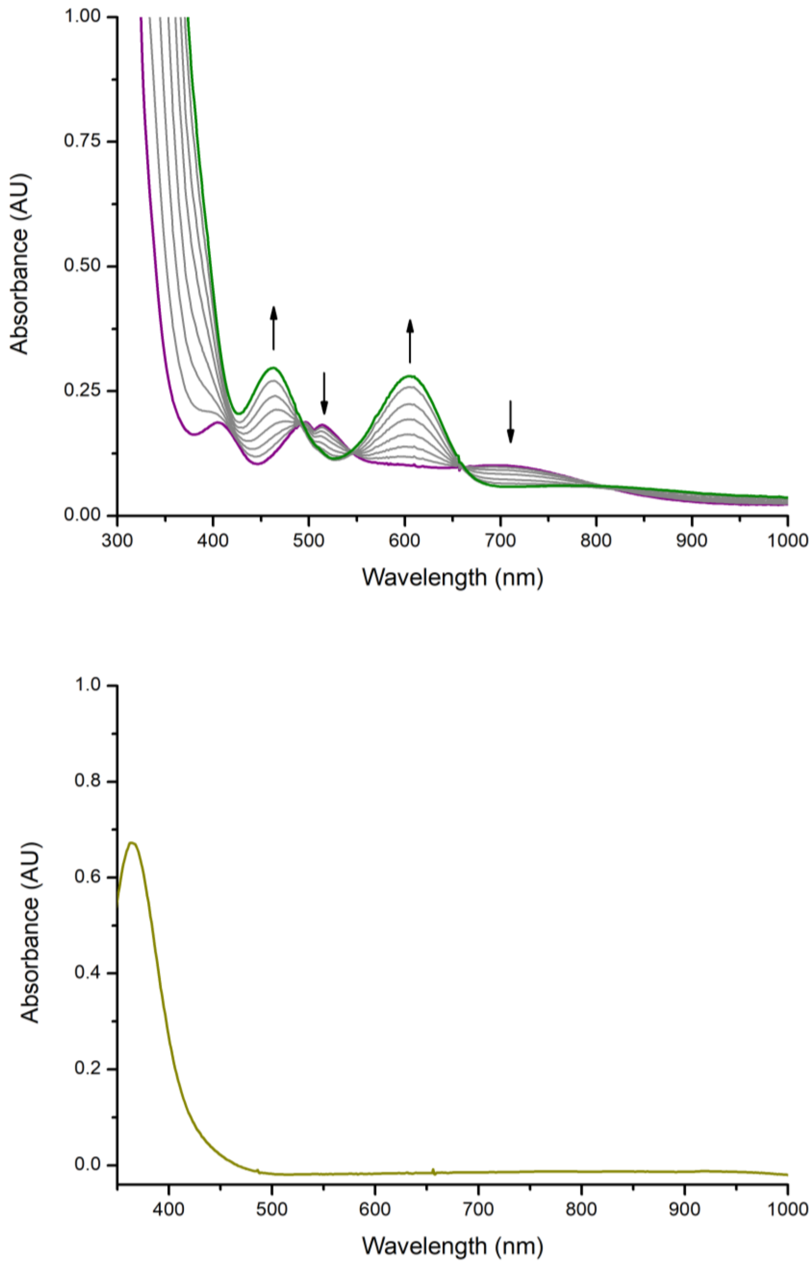

Figure S11. (a) Reaction of **5** with one equiv of HOTf in THF forming [Mn(BDPP)(H_2O)]OTf (**6**), which was subsequently warmed up. (b) 100 µL of the resulting solution was added into an acetone solution of excess NaI to examine the yield of the produced H_2O_2. The theoretical concentration of the in situ generated I_3^- solution is 3.2×10^{-5} M. The amount of the formed I_3^- was then quantified using its visible spectrum (λ_{max} = 361 nm, $\varepsilon = 2.5 \times 10^4$ M^{-1} cm^{-1}).

(a)

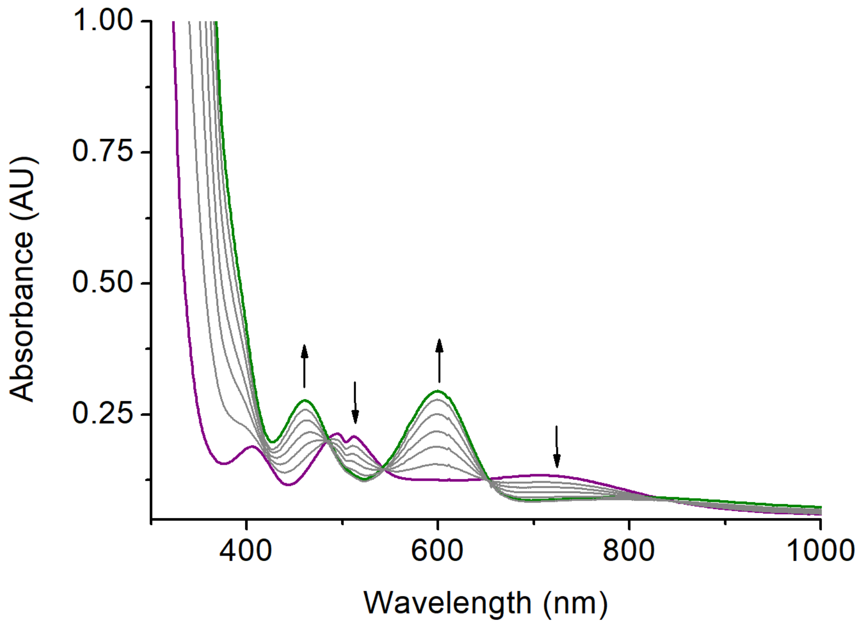

(b)

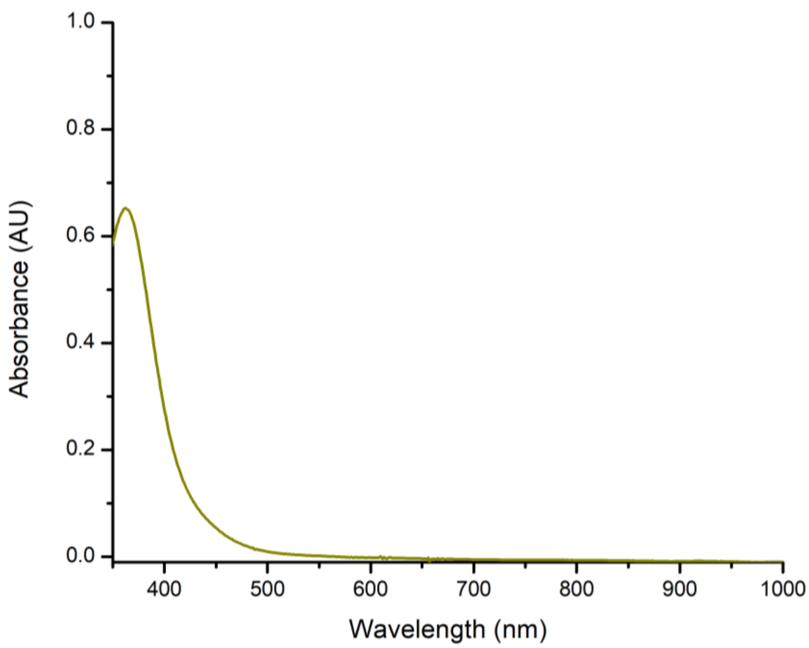

Figure S12. (a) Reaction of **5′** with one equiv of HOTf in THF forming [Mn(BDP^{Br}P)(H_2O)]OTf (**6′**), which was subsequently warmed up. (b) 100 µL of the resulting solution was added into an acetone solution of excess NaI to examine the yield of the produced H_2O_2. The theoretical concentration of the in situ generated I_3^- solution is 3.2×10^{-5} M. The amount of the formed I_3^- was then quantified using its visible spectrum (λ_{max} = 361 nm, $\varepsilon = 2.5 \times 10^4$ M^{-1} cm^{-1}).

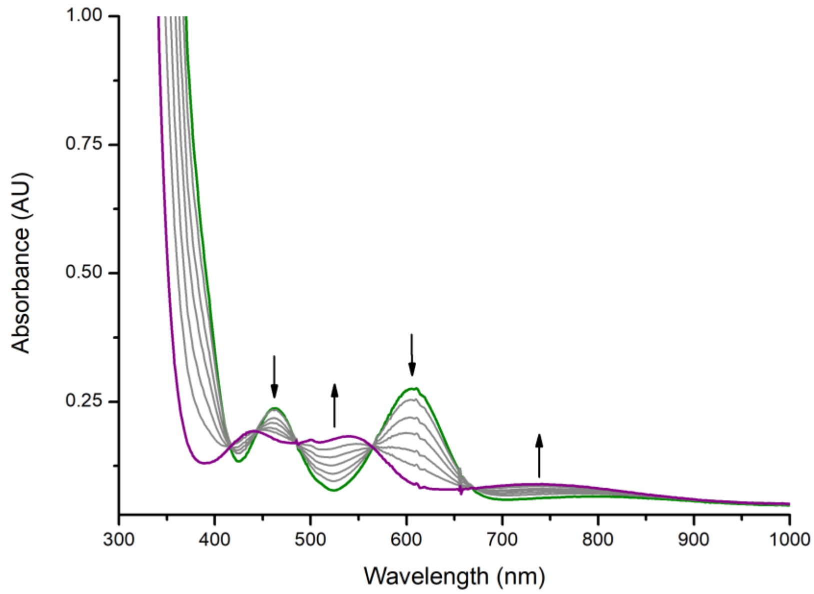

Figure S13. UV-vis spectra change monitored from the reaction of [Mn(BDPP)(H_2O)]OTf (**6**) (green line, 1 mM) with excess H_2O_2/NEt_3 2:1 mixture in THF at −90 °C. The purple line represents Mn(BDPP)(OOH) (**5**).

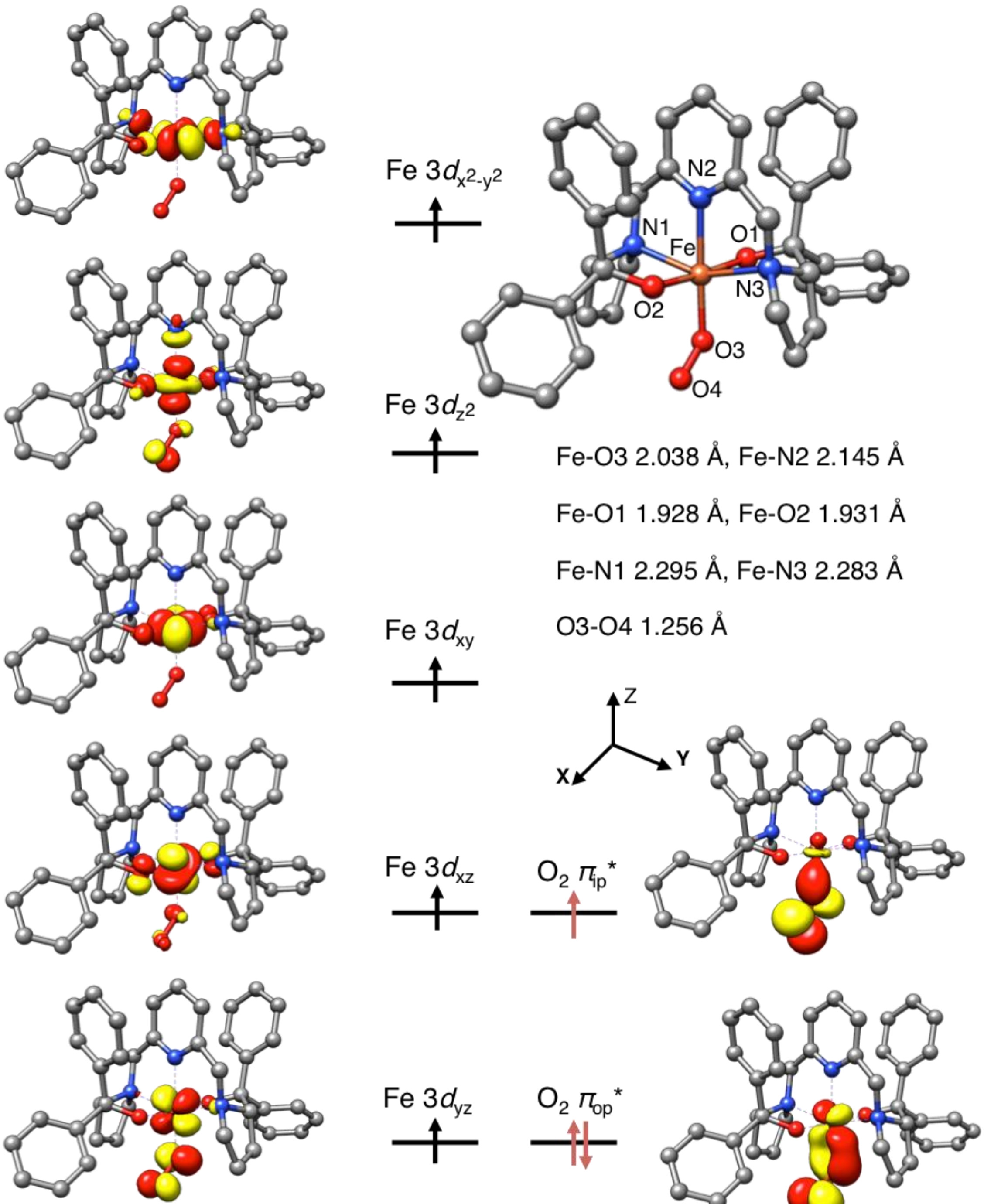

Figure S14. Computed structure of S = 3 Fe^{III}-superoxo **3** with key geometric parameters and its schematic molecular orbital diagram.

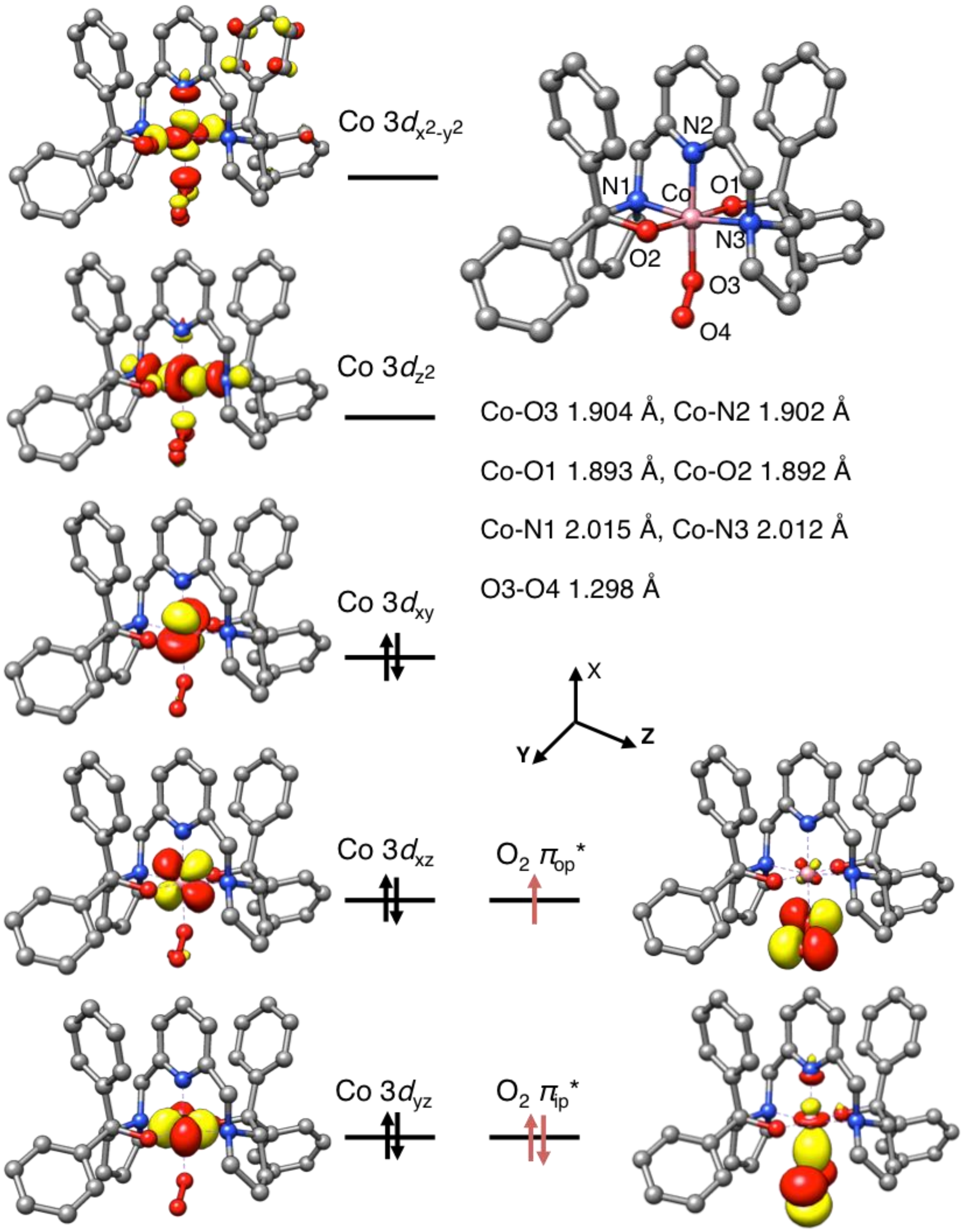

Figure S15. Computed structure of S = ½ Co^{III}-superoxo **4** with key geometric parameters and its schematic molecular orbital diagram.

For most transition metal complexes, the zero-field splitting arises from 2nd order spin-oribit coupling between the ground and excited states. A negative *D* value is usually found for a high spin d^4 center in a elongated octahderal coordination environment, because

$$D = -\frac{1}{4}\frac{\zeta^2}{\Delta\left({}^5B_{2g}\right)} + \frac{1}{16}\frac{\zeta^2}{\Delta\left({}^5E_g\right)} - \frac{1}{4}\frac{\zeta^2}{\Delta\left({}^3E_g\right)}$$

here ζ is the effective spin-orbit coupling constant of the metal center, Δ is the excitation energy of a given excited state.

The hyperfine coupling constant (HFC) is predicted to display a pattern of $|A_{x,y}| > |A_z|$, because

$$A_z = A^{FC} + \frac{4}{7}kP$$

$$A_{x,y} = A^{FC} - \frac{2}{7}kP$$

here A^{FC} is the Fermi-contact contribution to the HFC and is always negative for mononuclear transition metal complexes, $\kappa < 1$ is the orbital reduction factor and P is the proportional constant of the nucleus and is negative for ^{55}Mn. Because the intrinsic g values of **2** and **2′** are very close to 2, the orbital contribution to the HFC is negligible.

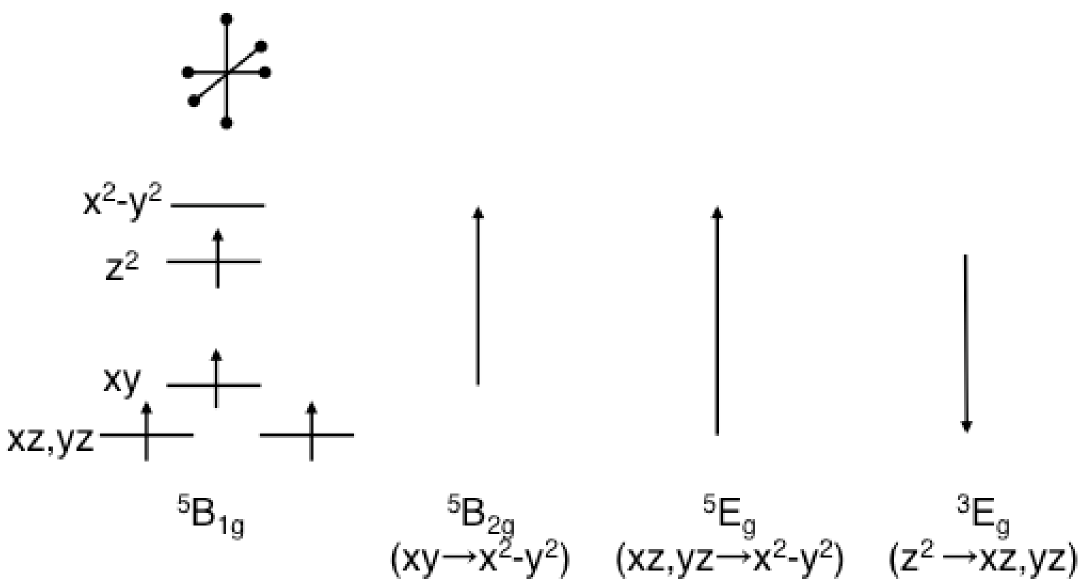

Figure S16. Correlation of the coordination geometry of **2′** with its spin Hamiltonian parameters. The ground state of a high spin d^4 center in a elongated octahderal coordination environment and low-lying excited states in D_{4h} symmetry.

A kinetic titration with ~2 × 10^{-4} M of **2′** and TEMPOH at 1.0, 1.5, 2.0, 2.5 equivalent concentrations was performed. All these numbers are based on a 100% yield in their preparation processes. The concentration of **2′** was corrected to 1.86 × 10^{-4} M using the EPR data (~93% yield, Figure S10), while the concentrations of TEMPO-H remained unknown. We then performed a titration with the nominal 1.0, 1.5, 2.0, 2.5 equiv of TEMPO-H and fitted to the kinetic model to obtain the actual value of *n* and rate constant, *k*. The actual value of *n* against the nominal *n* was plotted and we found that the yield of TEMPO-H generation was ~80%, which is consistent with the value extracted from the ^{1}H NMR spectrum (Figure S18). Therefore, the actual amount of the employed TEMPO-H is 0.8, 1.2, 1.6, and 2.0 equivalents, respectively.

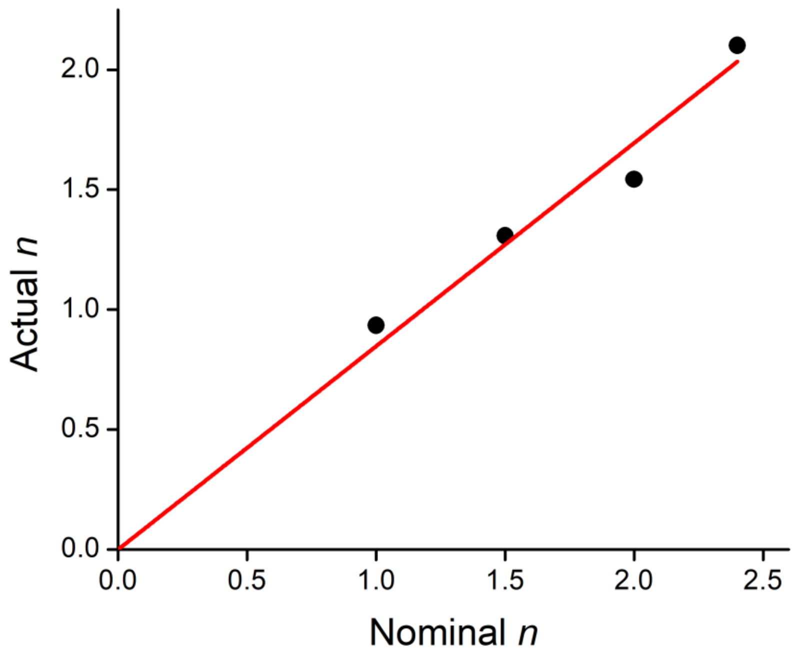

Figure S17. The linear plot of the actual value of *n* against the nominal *n*.

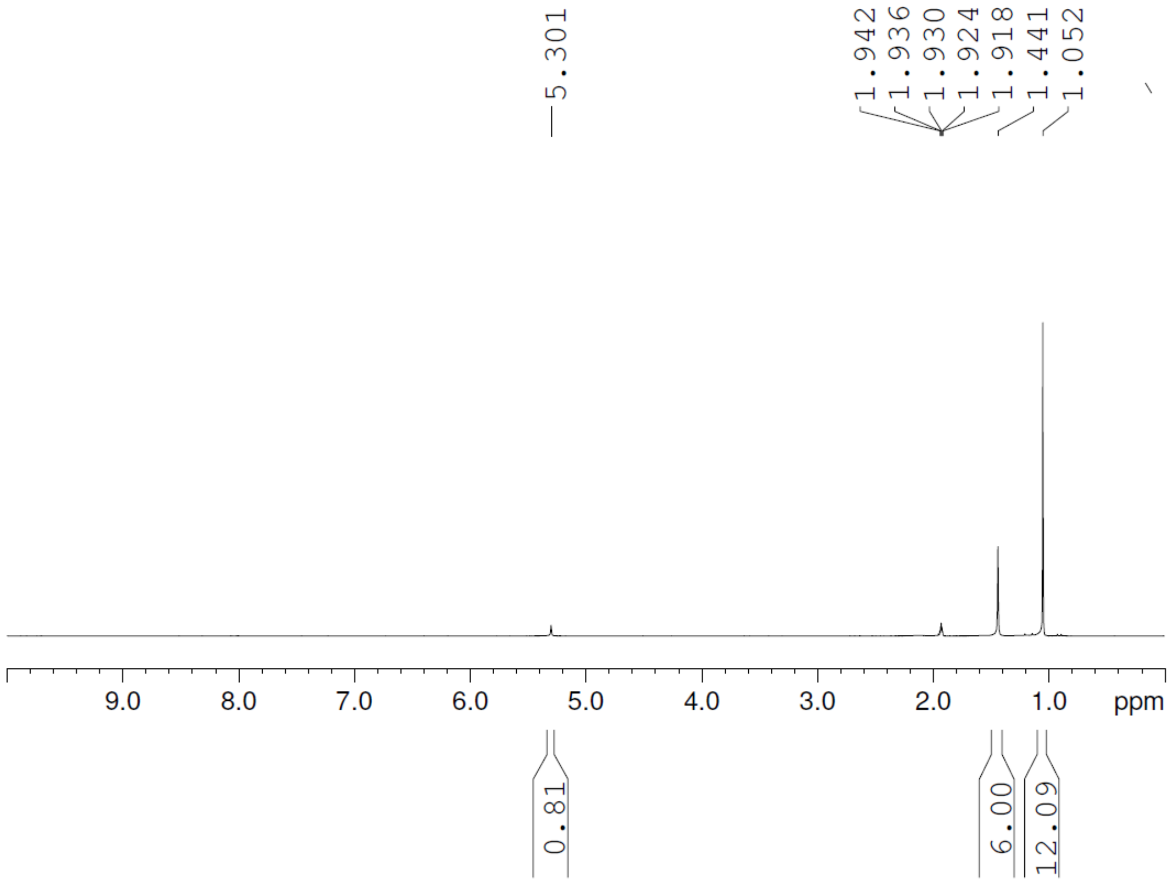

Figure S18. ^{1}H NMR spectrum of the prepared TEMPO-H in CD_3CN.

Table S1. Mn-O bond distances of Mn-(O_2), Mn-OOR, and Mn-OR (R = H, Me, Ph, Ph-$^{p}NO_2$) complexes.

Complex	Mn-O (Å)	ref.
$[Mn(O_2)(TPP)]^-$	1.888/1.901	*2*
$[Mn(O_2)(Tp^{iPr2})(pz^{iPr2})]$	1.850/1.851(brown) 1.841/1.878(blue)	*3*
$Tp^{iPr2}Mn(\eta^2\text{-}O_2)(im^{Me}H)$	1.872 /1.838	*4*
$[Mn(O_2)(TMC)]^+$	1.884	*5*
$[Mn(O_2)(13\text{-}TMC)]^+$	1.855 / 1.863	*6*
$[Mn(O_2)(12\text{-}TMC)]^+$	1.853	*7*
$[Mn^{III}(OO^tBu)(S^{Me2}N_4(QuinoEN))]^+$	1.861	*8*
$[Mn^{III}(OOCm)(S^{Me2}N_4(QuinoEN))]^+$	1.841	*8*
$[Mn^{III}(OO^tBu)(S^{Me2}N_4(QuinoPN))]^+$	1.840	*9*
$[Mn^{III}(OO^tBu)(S^{Me2}N_4(6\text{-}Me\text{-}DPEN))]^+$	1.853	*9*
$[Mn^{III}(OOCm)(S^{Me2}N_4(6\text{-}Me\text{-}DPEN))]^+$	1.848	*9*
$[Mn^{III}(OO^tBu)(S^{Me2}N_4(6\text{-}Me\text{-}DPPN))]^+$	1.843	*9*
$[Mn_2^{III}(\textit{trans}\text{-}1,2\text{-}O_2)(S^{Me2}N_4(6\text{-}Me\text{-}DPEN))_2]^{2+}$	1.832	*10*
$[Mn^{III}(S^{Me2}N_4(tren)(OPh\text{-}^{p}NO_2))]^+$	1.901	*11*
$[Mn^{III}(S^{Me2}N_4(tren)(OPh))]^+$	1.867	*11*
$[Mn^{III}(S_{Me2}N_4(tren)(OMe))]^+$	1.836	*11*
$[Mn^{III}(S_{Me2}N_4(tren))(OH)]^+$	1.854	*11*

Table S2. The O-O bond length of metal-superoxo complexes.

complex	O-O (Å)	ref.
$[Cu^{II}(TMG_3tren)(\eta^1\text{-}O_2^{\bullet})]^+$	1.280(3)	*12*
$[Cr^{III}(14\text{-}TMC)(O_2)(Cl)]^+$	1.231(6)	*13*
$[Fe^{III}(TAML)(O_2)]^{2-}$	1.323(3) / 1.306(7)	*14*
$Co^{III}(Tp^{Me2})(L^{Ph})(O_2^{\bullet})$	1.301(5)	*15*

Table S3. Computed Spectroscopic Parameters for **2′** and **5′**.

	2′	**5′**
D (cm^{-1}), E/D	–3.1, 0.08	–2.8, 0.11
$A_{x,y,z}$ (MHz)	–194, –183, –60	–166, –164, –47

Table S4. Metal-superoxo bond lengths of mononuclear metal superoxo complexes by the B3LYP calculations

Complex	Metal-O (Å)
$Mn^{III}(BDPP)(O_2^{\bullet})$ (**2**) $S = 3/2$	1.932
$Mn^{III}(BDP^{Br}P)(O_2^{\bullet})$ (**2′**) $S = 3/2$	1.937
$Fe^{III}(BDPP)(O_2^{\bullet})$ (**3**) $S = 3$	2.038
$Fe^{III}(BDPP)(O_2^{\bullet})$ $S = 2$	1.927
$Co^{III}(BDPP)(O_2^{\bullet})$ (**4**) $S = 1/2$	1.904

For **2**, **2′** and **4**, the strongly antibonding σ* orbital with respect to the metal-superoxo interaction is vacant (Fig. 2, S15 and S16), but it is singly occupied for **3** (S15). In fact, the computed Fe-superoxo bond distance for the quintet state of **3**, which contains a high spin ferric center antiferromagnetic coupled to a superoxo radical, is comparable to those estimated for **2**, **2′** and **4**. This observation reflects the tradeoff between the enhanced Lewis acidity of Fe^{III} relative to Mn^{III} and the different occupation of the σ* orbital. Thus, the weaker metal-superoxo bonding in **3** arises from the synergistic effect of its high spin center and the ferromagnetic coupling between the metal center and the superoxo ligand.[16]

Table S5. Coordinates of the optimized structures:

$Mn^{III}(BDPP)(O_2^{\bullet})$ (**2**):

Mn	−1.49310707853518	10.62070401636536	8.32599976055327
H	−0.84052727955616	17.89033641991843	10.90627631645225
H	5.01857969650649	11.26080589118739	10.73402742227351
H	2.07503813535693	4.69710544057160	7.17726564893587
H	−6.52629979160194	5.68105357315492	5.16186779040529
O	−3.24166978381150	11.38799509030409	8.02900524329407
O	−3.67414027267409	12.38540561576013	8.73889422220261
C	0.14622534588044	12.91909531175147	8.89420317066122
C	−0.10175819939280	14.32777139554240	9.48067608502189
C	−1.25039677166967	14.56342102057798	10.24525422320290
H	−1.93956318762866	13.73466405363135	10.40731447700653
C	−1.51079762708346	15.83900015954261	10.75611094238972
H	−2.41295124351058	16.01080940148165	11.34932715597300
C	−0.63111416155302	16.89485978040468	10.50572522119420
C	0.51685892349555	16.66620033960102	9.74001798282374
H	1.21463140476065	17.48265789959905	9.53463229871925
C	0.78122712437718	15.38973374736062	9.23787936590845
H	1.68990679752214	15.22651825550652	8.65561492712120
C	1.54887194262492	12.46969719222107	9.36596705764002
C	2.73958683059272	12.79531667872422	8.70057964326542
H	2.71500331928337	13.37736517287429	7.77844432724151
C	3.97994414641610	12.36899942252690	9.18659308766635
H	4.88957689851170	12.63625731700067	8.64209549326547
C	4.05404321691218	11.60804093254889	10.35443668331921
C	2.87486989710584	11.29685339035780	11.04027114237799
H	2.92024551233145	10.70946489236244	11.96124903998786
C	1.64258364048388	11.73112271640251	10.55379545548812
H	0.71758323045842	11.49274445394469	11.07828216750919
C	0.03054424875374	13.01350794885808	7.33871011130346
H	0.92560174913585	13.49914005568553	6.91415736805470
C	−1.22935184923215	13.78141861355586	6.88475407665857
H	−1.97189364236985	13.79093638171272	7.69038637713665

H	−0.97223894775023	14.82627823552659	6.66723557592898
C	−1.77725422560312	13.02753657281822	5.65407694949191
H	−2.75641374083611	12.58670119431629	5.88264408708293
H	−1.89349957099467	13.67868948992305	4.77560516984310
C	−0.75659811348951	11.92502328627028	5.39325748774536
H	0.01636172848060	12.26694458237399	4.67525449574295
H	−1.19829923760710	10.99144994844540	5.01360615265501
C	1.06911767983923	10.84907647110080	6.56677054854184
H	1.95803285176790	11.45646027571068	6.31653191108363
H	0.89929909586749	10.17687255315494	5.70992296512588
C	1.37718178772157	9.94743723234859	7.73670328778378
C	2.63036273687908	9.35639310753699	7.89098221968994
H	3.44894682225362	9.63872870375137	7.22748523312434
C	2.80255281499032	8.40870985846851	8.89768697164028
H	3.76845122084391	7.91949326496361	9.03974231178131
C	1.73067134844477	8.09084462052730	9.72844525722570
H	1.82770650367504	7.34300276009553	10.51720185330483
C	0.52183339522911	8.76020374383102	9.54559777832321
C	−0.62042152643410	8.60130967639636	10.51590417775830
H	−0.66663788248012	7.55661159889587	10.87325597294391
H	−0.35694430627211	9.21816904305559	11.39034391872744
C	−2.74101448079485	9.55216783923231	11.17267865456405
H	−2.35186068527505	10.52434641557261	11.50887011882127
H	−2.65827114126878	8.83461371509353	12.01292500613640
C	−4.17621664612315	9.60827754301264	10.64886547286976
H	−4.44157906791470	10.63166304101441	10.35420249288793
H	−4.88441878685141	9.28416969140637	11.42500795408573
C	−4.18950268671887	8.67571007509249	9.42026330828641
H	−4.43180365654426	9.24320804804754	8.51485526213079
H	−4.92545405682129	7.86561554583102	9.50545123073820
C	−2.77069760270976	8.08653454225467	9.30624534264463
H	−2.73621451277729	7.12167837903978	9.83941099533761
C	−2.31040895284103	7.90001149803476	7.82128606759063
C	−1.07750853439159	6.97291040085040	7.68970790982256
C	−0.17128687132606	7.21511137761188	6.64631592956467

H	−0.36474146799768	8.06470797694014	5.99178428969691
C	0.95143468263482	6.40845123817842	6.46143894261341
H	1.64565259605728	6.62661718534472	5.64537207714192
C	1.19475073916931	5.32914432652405	7.31853980673017
C	0.29061294423970	5.06106776063986	8.34797061782119
H	0.45851731829559	4.21467797376120	9.01920607693330
C	−0.83338430907712	5.87509834869954	8.52874505418955
H	−1.52070652810445	5.64004213160069	9.34287847250619
C	−3.47360557149796	7.23740549304771	7.04698724005872
C	−3.94687175692993	5.96061622361439	7.38178550972141
H	−3.46126792055097	5.38588801440165	8.17257289458921
C	−5.04258777707580	5.40654561529835	6.71644512752867
H	−5.40984463131399	4.41920776592237	7.00850828330096
C	−5.67193196848414	6.11499857852955	5.68738552998992
C	−5.19788026001982	7.38186899170038	5.33982568349371
H	−5.68621831426943	7.94838012985158	4.54232610685194
C	−4.11182467742997	7.94251536066904	6.02026925654814
H	−3.74931301861282	8.94133408108303	5.77955364122230
N	−0.13031332963904	11.67191750508400	6.70888526860159
N	0.37594260786863	9.65378823960454	8.56720800832749
N	−1.92108157411194	9.06864407721198	10.03754111049954
O	−0.83880228711981	12.04660752668565	9.35677533812856
O	−2.04512742008841	9.15377754296478	7.27301730742646

$Mn^{III}(BDP^{Br}P)(O_2^{\bullet})$ (**2′**):

Mn	−1.51895213447833	10.63764487741676	8.38349320521501
Br	−0.69886924630518	18.67328640191320	11.34082736319431
Br	5.83028820189951	11.36773456966083	11.04635755294360
Br	2.56450232421277	4.10185962226560	6.86817348804085
Br	−7.04650463447380	5.32476516131998	4.52275941149838
O	−3.25046321243856	11.46928666281454	8.13180343235474
O	−3.70563578810636	12.23377387734376	9.07203661888293
C	0.16403311485209	12.98555612225928	8.84722230288068
C	−0.07967251569240	14.41405533912043	9.40893584770970

C	−1.14945432086786	14.65182633004714	10.28131256437410
H	−1.82859676885991	13.82872577998237	10.50831593980150
C	−1.34886562116418	15.91552360797323	10.84999674238523
H	−2.18025612174042	16.08700596102225	11.53671489706009
C	−0.47157408926745	16.95524776419527	10.53618233400430
C	0.58395009786854	16.75192216605784	9.64282181859021
H	1.25928086704623	17.57127996901351	9.38945836919177
C	0.77557710807385	15.48289661721714	9.09433367005859
H	1.62491870271034	15.33539653698615	8.42407692688164
C	1.58896229011548	12.59263542189372	9.33945946164418
C	2.77233638691858	12.90972316384025	8.65343135039126
H	2.73877140470569	13.43117095736294	7.69547177903210
C	4.03164490604418	12.56340866797068	9.15513013643115
H	4.93424262047361	12.81643446378240	8.59591219812835
C	4.12056971861702	11.89000717167201	10.37276009886100
C	2.96332172004586	11.59097211465942	11.09806655048970
H	3.03874811976159	11.07961871509721	12.05948095232366
C	1.71680208039033	11.94723493165507	10.57986661930432
H	0.80930801088285	11.71676691565925	11.13995191228821
C	0.03915535867764	13.01807686338296	7.28430485676101
H	0.93392518274367	13.48158333401761	6.83245170734228
C	−1.21792363020898	13.77610768830851	6.79106910805497
H	−1.97154596558760	13.82366672656190	7.58641731724972
H	−0.95650898762018	14.81123195254483	6.53254665537519
C	−1.75507939939716	12.98006021293985	5.57936828791997
H	−2.73844916999840	12.54759768381982	5.81040592321553
H	−1.86396403763088	13.60179200678189	4.67842686101875
C	−0.72959721525393	11.86969403675116	5.36723571121618
H	0.05678616732264	12.19402589379667	4.65513599591034
H	−1.16526075428505	10.92927984698939	4.99670449383439
C	1.06456732236963	10.80229164895816	6.60948810095341
H	1.96510751655431	11.38854198747787	6.34802322656000
H	0.89775089738668	10.10765300890686	5.76953491118417
C	1.35690506111960	9.92536409352627	7.81073801149918
C	2.61400521721329	9.34588580703825	7.99504132921536

H	3.43755478309707	9.60684445798512	7.32763960927968
C	2.78905786223767	8.43842633039606	9.03964476958529
H	3.76115559140527	7.97116587299995	9.21234661463829
C	1.70944611929002	8.13387575382380	9.86716390001944
H	1.81094277550215	7.41776407882897	10.68539352730576
C	0.48770589893565	8.77217970270913	9.64109699885035
C	−0.67704941577576	8.58453665479576	10.58838263871250
H	−0.70106651169894	7.53703303114839	10.94380607193627
H	−0.44322248354237	9.19857143792281	11.47409081902687
C	−2.82894904484766	9.43686618944339	11.26576831970328
H	−2.50068100016645	10.42788558044328	11.61231037992928
H	−2.67910689732079	8.71703005504197	12.09432528065135
C	−4.28317353294754	9.40310568190992	10.78605524801321
H	−4.66293109921776	10.41753699631108	10.60648219931047
H	−4.92761456753490	8.93523755851250	11.54522614532995
C	−4.25137465425307	8.59519255547742	9.47272899061343
H	−4.46709505971736	9.24928168863843	8.61901106359643
H	−4.98745001341148	7.78032947671982	9.45261854915960
C	−2.82204722955437	8.03287118155913	9.34379760153004
H	−2.77193805417610	7.05851950951650	9.86221153172001
C	−2.36899017132657	7.88158179381403	7.84438629947087
C	−1.15015452108834	6.92807294256801	7.66505992698906
C	−0.29887676309092	7.13137539814572	6.56569279557274
H	−0.50574296367005	7.97239482930868	5.90219469883847
C	0.79096877956919	6.29654688387751	6.31348472205533
H	1.44155309388061	6.47991672329246	5.45600937915007
C	1.04948024773455	5.22483895923977	7.17481211930087
C	0.20552291674337	4.97418191488065	8.25721393078768
H	0.39535545874947	4.12868671469919	8.92097426299395
C	−0.88317966505510	5.82384762614396	8.49076087158757
H	−1.52543088192492	5.59776636220494	9.34434093633718
C	−3.52991698724387	7.23409099348480	7.03331364605176
C	−4.00338240857447	5.94261230991513	7.31682230478371
H	−3.55285075377401	5.35180342299150	8.11747270517795
C	−5.04901918301018	5.37268180070748	6.58701894684947

H	−5.41233656423509	4.37268829902008	6.83092442008144
C	−5.62508382597893	6.09723013056092	5.53905436694107
C	−5.17122740896267	7.38067065068941	5.23323664242497
H	−5.63006793937309	7.94465116644820	4.41885126476371
C	−4.13235311616938	7.94154370325136	5.98483328970997
H	−3.77763327829933	8.94864361278806	5.76512122999060
N	−0.12927467238321	11.64914899284981	6.70523673792535
N	0.34548613162024	9.64321773996093	8.63886387226109
N	−1.99276732827259	9.02274485528116	10.10428925422039
O	−0.80063127784808	12.11167705041748	9.34577880317703
O	−2.09516616894922	9.14875864727107	7.33209727237414

Fe^{III}(BDPP)($O_2^{\bullet}$) (**3**) (*S* = 3):

Fe	1.951648	3.352647	18.365824
O	0.285517	4.462169	18.745998
O	−0.876834	4.759570	19.116170
O	2.833465	4.863863	17.547830
O	1.052787	1.817025	19.106950
N	1.653766	2.798412	16.170781
N	3.669333	2.136842	17.951469
N	3.020375	3.255953	20.393969
C	3.042481	4.906006	16.174129
C	2.997345	6.366250	15.668693
C	2.936758	7.410335	16.596526
H	2.896584	7.152372	17.655029
C	2.919853	8.742954	16.171503
H	2.876557	9.546315	16.911940
C	2.952216	9.051074	14.809845
H	2.936610	10.091720	14.474851
C	3.003469	8.013182	13.874669
H	3.027005	8.240881	12.805231
C	3.032844	6.684384	14.302147
H	3.088284	5.893503	13.551646
C	4.454263	4.384669	15.804342

C	4.795061	3.908142	14.529605
H	4.042074	3.845946	13.742822
C	6.100729	3.504588	14.233239
H	6.340118	3.126322	13.235452
C	7.097121	3.577918	15.207811
H	8.116343	3.257351	14.976144
C	6.773102	4.066065	16.478105
H	7.545431	4.138159	17.248550
C	5.467992	4.464441	16.768845
H	5.201173	4.849526	17.753066
C	1.897733	4.097529	15.479969
H	2.140652	3.889842	14.423606
C	0.540784	4.819309	15.562749
H	0.550594	5.520788	16.405916
H	0.370903	5.411265	14.654557
C	−0.525014	3.722580	15.777061
H	−1.071251	3.895062	16.712317
H	−1.267050	3.691865	14.965672
C	0.260156	2.411271	15.839734
H	−0.104990	1.710130	16.604147
H	0.247036	1.898581	14.858410
C	2.582778	1.703648	15.849439
H	2.030040	0.761840	15.998436
H	2.891602	1.733006	14.789673
C	3.794725	1.605775	16.740032
C	4.942230	0.897190	16.386978
H	5.059221	0.495760	15.379724
C	5.925482	0.708761	17.357336
H	6.825974	0.139606	17.116403
C	5.751541	1.244894	18.633604
H	6.498195	1.093230	19.415130
C	4.601447	1.994393	18.885812
C	4.392502	2.768175	20.167098
H	5.040078	3.656274	20.092044
H	4.757724	2.185440	21.030630

C	3.055264	4.540085	21.137136
H	3.417279	5.334204	20.467785
H	3.758516	4.451924	21.988932
C	1.628745	4.749664	21.636718
H	1.055628	5.350918	20.920507
H	1.618684	5.281096	22.598995
C	1.038065	3.327979	21.735414
H	0.775763	3.045185	22.763629
H	0.121751	3.257080	21.141224
C	2.109070	2.364306	21.182042
H	2.682118	1.934540	22.021312
C	1.487167	1.234272	20.289767
C	2.475360	0.081993	19.998586
C	2.332752	−0.604720	18.783724
H	1.542683	−0.279014	18.106028
C	3.181924	−1.656780	18.444243
H	3.053287	−2.170806	17.487793
C	4.195135	−2.058416	19.322282
H	4.865068	−2.879456	19.054820
C	4.331964	−1.403157	20.546736
H	5.108321	−1.711114	21.252251
C	3.475098	−0.348176	20.881859
H	3.607946	0.141041	21.847862
C	0.281219	0.630910	21.046256
C	0.435500	−0.184631	22.175498
H	1.432901	−0.452694	22.528199
C	−0.679293	−0.685683	22.852910
H	−0.536486	−1.323716	23.729311
C	−1.968730	−0.374115	22.411408
H	−2.839526	−0.767652	22.941745
C	−2.130114	0.439420	21.285979
H	−3.131925	0.697205	20.930614
C	−1.013508	0.934236	20.607039
H	−1.122109	1.566035	19.725039

$Fe^{III}(BDPP)(O_2^{\bullet})$ (S = 2):

Fe	1.909703	3.383413	18.376237
O	0.365561	4.489157	18.699610
O	−0.775402	4.154883	19.184275
O	2.855915	4.850910	17.555327
O	1.064975	1.824708	19.099184
N	1.624922	2.818869	16.190800
N	3.635978	2.161124	17.956186
N	2.994223	3.289285	20.382581
C	3.057850	4.895736	16.179487
C	3.028399	6.358998	15.681632
C	2.955700	7.400104	16.611682
H	2.896735	7.139749	17.668638
C	2.949081	8.733844	16.189768
H	2.896020	9.535270	16.931631
C	3.003313	9.045495	14.829583
H	2.995790	10.087052	14.497154
C	3.066519	8.010149	13.892279
H	3.107961	8.240761	12.824021
C	3.086481	6.680305	14.316728
H	3.153008	5.890655	13.565919
C	4.460140	4.359650	15.797812
C	4.781836	3.864446	14.525222
H	4.017817	3.792817	13.749899
C	6.082439	3.453914	14.216279
H	6.306620	3.061223	13.220597
C	7.092637	3.538265	15.175512
H	8.107864	3.212537	14.933786
C	6.787497	4.044507	16.443488
H	7.570732	4.125974	17.201879
C	5.487657	4.450676	16.746652
H	5.236587	4.853051	17.728181
C	1.895054	4.109164	15.490955
H	2.134642	3.886594	14.437121

C	0.552013	4.858120	15.564311
H	0.571297	5.563782	16.403378
H	0.397664	5.445519	14.650277
C	−0.535150	3.783476	15.784442
H	−1.076674	3.968451	16.720033
H	−1.275500	3.760239	14.971228
C	0.223178	2.457556	15.860604
H	−0.157561	1.771430	16.630926
H	0.204900	1.935079	14.884896
C	2.532405	1.705075	15.873799
H	1.967993	0.774067	16.043928
H	2.827492	1.716177	14.809946
C	3.751115	1.611064	16.752705
C	4.894203	0.895293	16.400344
H	5.001310	0.478532	15.398320
C	5.886942	0.722309	17.363638
H	6.784936	0.149119	17.123241
C	5.725277	1.280048	18.632230
H	6.479040	1.141520	19.409309
C	4.577521	2.032918	18.882970
C	4.374404	2.826839	20.150752
H	5.001652	3.726626	20.049876
H	4.758331	2.267881	21.021797
C	3.006639	4.578652	21.119923
H	3.339640	5.376598	20.440144
H	3.725146	4.511091	21.960286
C	1.583243	4.755027	21.639440
H	0.985005	5.332924	20.924514
H	1.573450	5.293312	22.597790
C	1.028515	3.320278	21.754222
H	0.796101	3.033274	22.788421
H	0.102146	3.237236	21.178057
C	2.107280	2.378690	21.179253
H	2.701095	1.953579	22.005685
C	1.499398	1.242843	20.285375

C	2.496316	0.097079	19.999847
C	2.350764	−0.605683	18.794396
H	1.554673	−0.293946	18.117198
C	3.202836	−1.658084	18.463693
H	3.071792	−2.184479	17.514337
C	4.221305	−2.045072	19.342381
H	4.892561	−2.867430	19.082480
C	4.361469	−1.373626	20.557605
H	5.141820	−1.670082	21.263589
C	3.502485	−0.317337	20.883231
H	3.637635	0.183907	21.842728
C	0.290294	0.628915	21.029212
C	0.445036	−0.210528	22.140753
H	1.442463	−0.486426	22.487161
C	−0.669547	−0.724859	22.808882
H	−0.526039	−1.380910	23.671841
C	−1.958927	−0.404069	22.374225
H	−2.829803	−0.808474	22.896323
C	−2.120158	0.434090	21.266907
H	−3.121594	0.701590	20.917752
C	−1.004508	0.943683	20.597569
H	−1.117489	1.600593	19.735024

$Co^{III}(BDPP)(O_2^{\bullet})$ (**4**):

Co	−0.077080	−0.177359	0.993453
O	−0.258990	−0.663318	2.825244
O	0.231315	0.093113	3.758649
O	0.078293	1.674319	1.353370
O	−0.272041	−2.020381	0.611320
N	−2.045306	0.158401	0.719370
N	0.049713	0.153122	−0.875805
N	1.911880	−0.452879	0.870809
C	−1.027034	0.498075	−2.939850
C	−1.075789	0.261718	−1.568966

C	−2.299792	0.006411	−0.741522
C	−2.968079	−0.754285	1.458675
C	−3.137321	−0.168425	2.860228
C	−2.615563	1.280236	2.762915
C	−2.299512	1.537725	1.281785
C	−2.018398	4.701516	1.835953
C	−2.072141	5.769419	2.736160
C	−1.218165	5.797305	3.844148
C	−0.320714	4.744283	4.045219
C	−0.273970	3.672399	3.147912
C	−1.119333	3.643014	2.031497
C	−2.072400	3.311356	−1.183422
C	−1.911451	3.887715	−2.448854
C	−0.637357	4.206072	−2.919519
C	0.473364	3.954795	−2.106519
C	0.306002	3.381221	−0.847160
C	−0.966518	3.034074	−0.368043
C	−1.047054	2.438184	1.060376
C	0.227444	0.586037	−3.548015
C	1.390635	0.445190	−2.787853
C	1.256681	0.236266	−1.418835
C	2.356138	0.182643	−0.401260
C	2.668343	0.133956	2.035445
C	3.094036	−1.040969	2.920565
C	2.294273	−2.241512	2.408708
C	2.106140	−1.955461	0.920723
C	1.753827	−5.120935	0.427691
C	1.689050	−6.406919	0.970038
C	0.698522	−6.727022	1.904817
C	−0.219133	−5.748385	2.296256
C	−0.147967	−4.460343	1.757300
C	0.836478	−4.133365	0.816617
C	2.245045	−2.874162	−1.972223
C	2.277359	−3.022655	−3.363558
C	1.088383	−3.114240	−4.087316

C	−0.132188	−3.065853	−3.404858
C	−0.157185	−2.916869	−2.019181
C	1.028859	−2.804197	−1.277907
C	0.896127	−2.689463	0.262207
H	−1.944984	0.611657	−3.517540
H	−2.575937	−1.045427	−0.905548
H	−3.150784	0.629479	−1.058651
H	−3.935408	−0.764591	0.926515
H	−2.534163	−1.761571	1.430604
H	−4.192881	−0.215113	3.166958
H	−2.548948	−0.735646	3.590016
H	−3.337759	2.022058	3.127366
H	−1.704361	1.392765	3.357224
H	−3.192894	1.944081	0.781375
H	−2.671487	4.710510	0.961404
H	−2.775134	6.588976	2.560871
H	−1.249429	6.637883	4.543177
H	0.345218	4.751842	4.912726
H	0.405171	2.832740	3.297710
H	−3.082415	3.081797	−0.840790
H	−2.790306	4.095896	−3.064732
H	−0.508451	4.660272	−3.905043
H	1.474739	4.217039	−2.459677
H	1.160917	3.186191	−0.198020
H	0.300512	0.767580	−4.622339
H	2.377449	0.500495	−3.248944
H	2.622678	1.222591	−0.166717
H	3.254972	−0.317153	−0.795133
H	3.536333	0.690365	1.653816
H	1.996805	0.834895	2.545026
H	4.175123	−1.226990	2.808452
H	2.890453	−0.835621	3.980220
H	2.813207	−3.196335	2.560821
H	1.318017	−2.302976	2.901074
H	3.047406	−2.188242	0.397801

H	2.518641	−4.894414	−0.317914
H	2.409504	−7.165734	0.652668
H	0.640582	−7.734002	2.326067
H	−0.993565	−5.988359	3.030075
H	−0.843165	−3.677578	2.059632
H	3.193321	−2.815657	−1.436063
H	3.239202	−3.073881	−3.881112
H	1.110989	−3.239610	−5.172953
H	−1.070497	−3.153870	−3.958976
H	−1.101134	−2.884801	−1.473712

References

1. Aasa, R.; Vänngård, T. EPR Signal Intensity and Powder Shapes: A Reexamination. *J. Magn. Reson.* **1975**, *19* (3), 308–315.
2. VanAtta, R. B.; Strouse, C. E.; Hanson, L. K.; Valentine, J. S. Peroxo(tetraphenylporphinato)manganese(III) and chloro(tetraphenylporphinato)manganese(II) Anions. Synthesis, crystal Structures, and electronic Structures. *J. Am. Chem. Soc.* **1987**, *109*, 1425-1434.
3. Brown, P. M.; Caradoc-Davies, T. T.; Dickson, J. M. J.; Cooper, G. J. S.; Loomes, K. M.; Baker, E. N. Crystal Structure of a Substrate Complex of Myo-inositol Oxygenase, a Di-Iron Oxygenase with a Key Role in Inositol Metabolism. *Proc. Natl. Acad. Sci. U. S. A.* **2006**, *103*, 15032-15037.
4. Singh, U. P.; Sharma, A. K.; Hikichi, S.; Komatsuzaki, H.; Moro-oka, Y.; Akita, M. Hydrogen Bonding Interaction between Imidazolyl N–H Group and Peroxide: Stabilization of Mn(III)-Peroxo Complex $TpiPr_2Mn(\eta^2-O_2)$(imMeH) (imMeH=2-methylimidazole). *Inorg. Chim. Acta* **2006**, *359*, 4407-4411.
5. Seo, M. S.; Kim, J. Y.; Annaraj, J.; Kim, Y.; Lee, Y.-M.; Kim, S.-J.; Kim, J.; Nam, W. $[Mn(tmc)(O_2)]^+$: A Side-On Peroxido Manganese(III) Complex Bearing a Non-Heme Ligand. *Angew. Chem. Int. Ed.* **200**7, *46*, 377-380.
6. Annaraj, J.; Cho, J.; Lee, Y. M.; Kim, S. Y.; Latifi, R.; de Visser, S. P.; Nam, W. Structural Characterization and Remarkable Axial Ligand Effect on the Nucleophilic Reactivity of a Nonheme Manganese(III)-Peroxo Complex. *Angew. Chem. Int. Ed.* **2009**, *48*, 4150-4153.
7. Kang, H.; Cho, J.; Cho, K. B.; Nomura, T.; Ogura, T.; Nam, W. Mononuclear Manganese-Peroxo and Bis(mu-oxo)dimanganese Complexes Bearing a Common N-Methylated Macrocyclic Ligand. *Chem. Eur. J.* **2013**, *19*, 14119-14125.
8. Coggins, M. K.; Kovacs, J. A. Structural and Spectroscopic Characterization of Metastable Thiolate-Ligated Manganese(III)-Alkylperoxo Species. *J. Am. Chem. Soc.* **2011**, *133*, 12470-12473.
9. Coggins, M. K.; Martin-Diaconescu, V.; DeBeer, S.; Kovacs, J. A. Correlation Between Structural, Spectroscopic, and Reactivity Properties Within a Series of Structurally Analogous Metastable Manganese(III)-Alkylperoxo Complexes. *J. Am. Chem. Soc.* **2013**, *135*, 4260-4272.
10. Coggins, M. K.; Sun, X.; Kwak, Y.; Solomon, E. I.; Rybak-Akimova, E.; Kovacs, J. A. Characterization of Metastable Intermediates Formed in the Reaction Between a Mn(II) Complex and Dioxygen, Including a Crystallographic Structure of a Binuclear Mn(III)-Peroxo Species. *J. Am. Chem. Soc.* **2013**, *135*, 5631-5640.

11. Coggins, M. K.; Brines, L. M.; Kovacs, J. A. Synthesis and Structural Characterization of a Series of Mn^{III}OR Complexes, Including a Water-Soluble Mn^{III}OH That Promotes Aerobic Hydrogen-Atom Transfer. *Inorg. Chem.* **2013**, *52*, 12383-12393.
12. Schatz, M.; Raab, V.; Foxon, S. P.; Brehm, G.; Schneider, S.; Reiher, M.; Holthausen, M. C.; Sundermeyer, J.; Schindler, S. Combined Spectroscopic and Theoretical Evidence For a Persistent End-On Copper Superoxo Complex. *Angew. Chem. Int. Ed.* **2004**, *43*, 4360-4363.
13. Cho, J.; Woo, J.; Nam, W. An "End-On" Chromium(III)-Superoxo Complex: Crystallographic and Spectroscopic Characterization and Reactivity in C−H Bond Activation of Hydrocarbons. *J. Am. Chem. Soc.* **2010**, *132*, 5958-5959.
14. Hong, S.; Sutherlin, K. D.; Park, J.; Kwon, E.; Siegler, M. A.; Solomon, E. I.; Nam, W. Crystallographic and Spectroscopic Characterization and Reactivities of a Mononuclear Non-Haem Iron(III)-Superoxo complex. *Nat. Commun.* **2014**, *5*, 5440-5447.
15. Oddon, F.; Chiba, Y.; Nakazawa, J.; Ohta, T.; Ogura, T.; Hikichi, S. Characterization of Mononuclear Non-heme Iron(III)-Superoxo Complex with a Five-Azole Ligand Set. *Angew. Chem. Int. Ed.* **2015**, *54*, 7336-7339.
16. Stout, H. D.; Kleespies, S. T.; Chiang, C. W.; Lee, W. Z.; Que, L., Jr.; Munck, E.; Bominaar, E. L., Spectroscopic and Theoretical Study of Spin-Dependent Electron Transfer in an Iron(III) Superoxo Complex. *Inorg. Chem.* **2016**, *55*, 5215-5226.